



# Basins of Attraction of Steady Operating Conditions in a Two-site Electricity and Heat Supply System

Hikaru Hoshino<sup>†</sup> Yoshihiko Susuki<sup>‡,§</sup> and Takashi Hikihara<sup>†</sup>

<sup>†</sup>Department of Electrical Engineering, Kyoto University  
Katsura, Nishikyo, Kyoto 615-8510 Japan

<sup>‡</sup>Department of Electrical and Information Systems, Osaka Prefecture University  
1-1 Gakuencho, Nakaku, Sakai, Osaka, 599-8513 Japan

<sup>§</sup>JST-CREST 4-1-8 Honcho, Kawaguchi, Saitama 332-0012 Japan

Email: hoshino@dove.kuee.kyoto-u.ac.jp, susuki@eis.osakafu-u.ac.jp, hikihara.takashi.2n@kyoto-u.ac.jp

**Abstract**—This paper analyzes the basin of attraction of a stable equilibrium point representing a steady operating condition of synchronous generators in a two-site electricity and heat supply system. The analysis is used for considering the effect of heat transfer management on the dynamics of the generators. The basin of attraction becomes small depending on the heat transfer rate, and a change of the set-points of the combined heat and power plants for regulating the heat transfer rate possibly destabilizes the generators.

## 1. Introduction

This paper numerically studies a dynamical model of two-site electricity and heat supply system based on our previous studies [1–3]. We examine the basin of attraction of a stable equilibrium point representing a steady operating condition of synchronous generators in the electric sub-system. This is of basic significance for understanding the system’s response to an open-loop control of the energy flows in the two-site system. In [3], we proposed a state-feedback (closed-loop) controller that enables regulation of electricity and heat flows based on the nonlinear control technique [4, 5]. This controller provides a trajectory of state variable which realizes the desired energy flows. However, it seems not easy to estimate the basin of attraction of the desired trajectory because of the complexity of the closed-loop system, in which the dynamics of the electric and heat sub-systems are coupled each other.

In this paper, we consider an open-loop control in which the set-points of Combined Heat and Power (CHP) plants (including gas turbines and generators) are already determined to realize the desired energy flows. To the open-loop control, the responses of the electric and heat sub-systems can be considered separately. In a viewpoint of dynamical systems theory, the studied model of the electric sub-system appears as a model of double swing dynamics with external forcing [6–8]. In [6–8], the basin structure of the model of swing dynamics was investigated by taking systematic slices of the phase space. In [9], a similar method for analyzing basin structure of dynamical systems is developed by using cell state space and mapping on it. Based on these studies, in [2], the basin portraits of the dynamical

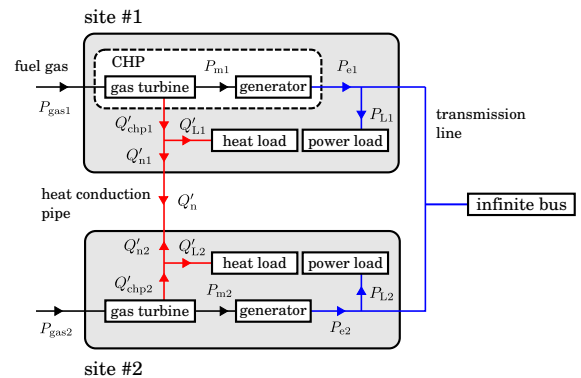


Figure 1: Block diagram of the two-site system. The arrows show the positive directions of energy flows.

cal model of the two-site system was visualized under several fixed values of the set-points of the CHP plants. The visualization was then used for understanding an ideal response of the two-site system to a step-wise change of the set-points of the CHP plants. Here, we discuss this in a more realistic situation, and consider a ramp-wise change of the set-points.

## 2. Mathematical model

This section introduces a dynamical model of the electricity and heat supply system based on [1, 2]. Figure 1 shows the block diagram of the two-site system in which the positive directions of energy flows are denoted. The notion of site is a unit of energy system that includes a CHP plant, power load, and heat load. The two sites are connected to an infinite bus through a transmission line and are interconnected by a heat conduction pipe.

### 2.1. Electric sub-system

The electric sub-system in Fig. 1 consists of the two generators, power loads, transmission lines, and infinite bus. The model of electric sub-system is based on the swing equation [10] with  $\delta_i$  representing the electric angular position of rotor with respect to the infinite bus, and  $\omega_i$  the

deviation of rotor speed relative to the synchronous speed  $\omega_s$ . The variable  $\delta_i$  is in the electrical radian, and  $\omega_i$  is scaled by  $\omega_r := \sqrt{\omega_s/2H_i}$ , where  $H_i$  stands for the per-unit time constant of rotor. The dynamics of generators are represented as follows: for  $i = 1, 2$ ,

$$\frac{d\delta_i}{dt} = \omega_i, \quad \frac{d\omega_i}{dt} = P_{mi} - D_i\omega_i - P_{ei}(\delta_1, \delta_2), \quad (1)$$

where  $P_{mi}$  stands for the mechanical input power to the generator, and  $D_i$  for the damping coefficient. The function  $P_{ei}$  stands for the electric output power and is given by

$$P_{ei} = \sum_{j \in \{1, 2, \infty\}} E_i E_j \{G_{ij} \cos(\delta_i - \delta_j) + B_{ij} \sin(\delta_i - \delta_j)\}, \quad (2)$$

with the symbol  $\infty$  representing the infinite bus, and  $\delta_\infty = 0$ . The parameter  $E_i$  corresponds to the voltage behind synchronous reactance, and  $G_{ij} + iB_{ij}$  are the transfer admittances.

## 2.2. Heat sub-system

The heat sub-system in Fig. 1 consists of the conduction pipe and loads. Here, we do not consider the transient dynamics and losses of heat transfer through the heat conduction pipe. This is relevant for considering the open-loop control of the two-site system. By using the following model, the set-points, i.e. the fuel inputs to the CHP plants, are determined to realize a desired heat transfer rate  $Q'_n$ . In Fig. 1, the conservation of energy at each site induces the following equality:

$$Q'_{\text{chpi}} = Q'_{ni} + Q'_{Li}. \quad (3)$$

Further, the heat output rates  $Q'_{n1}$  and  $Q'_{n2}$  satisfy

$$Q'_{n1} = -Q'_{n2} := Q'_n, \quad (4)$$

where  $Q'_n$  represents the heat transfer rate from site #1 to site #2.

## 2.3. Gas turbine

The gas turbine at site # $i$  converts the gas input rate  $P_{\text{gasi}}$  to both the mechanical power  $P_{mi}$  and the heat rate  $Q'_{\text{chpi}}$ . Because its time response is sufficiently fast compared with the electromechanical dynamics of the generators [11], the dynamics of the gas turbine are not considered in this paper. Then, the instantaneous conversion of energy at each gas turbine is represented by

$$\begin{bmatrix} P_{mi} \\ Q'_{\text{chpi}} \end{bmatrix} = \begin{bmatrix} \eta_{ei} \\ \eta_{hi} \end{bmatrix} P_{\text{gasi}}. \quad (5)$$

Throughout this paper, the parameters  $\eta_{ei}$  and  $\eta_{hi}$  are constant and satisfy  $\eta_{ei} + \eta_{hi} < 1$ . The constant  $\eta_{ei}$  represents the thermal efficiency of the gas turbine at site # $i$ , and  $\eta_{hi}$  the ratio of heat output rate to gas input rate.

## 2.4. Derived model

Consequently, the dynamics of the two-site electricity and heat supply system are represented by the following nonlinear dynamical model:

$$\frac{d\delta_1}{dt} = \omega_1, \quad (6a)$$

$$\frac{d\omega_1}{dt} = \frac{\eta_{e1}}{\eta_{h1}} (Q'_n + Q'_{L1}) - D_1\omega_1 - P_{e1}(\delta_1, \delta_2), \quad (6b)$$

$$\frac{d\delta_2}{dt} = \omega_2, \quad (6c)$$

$$\frac{d\omega_2}{dt} = \frac{\eta_{e2}}{\eta_{h2}} (-Q'_n + Q'_{L2}) - D_2\omega_2 - P_{e2}(\delta_1, \delta_2). \quad (6d)$$

The dynamical model (6) contains the parameters  $Q'_n$  and  $Q'_{Li}$  of the heat sub-system. In the rest of this paper, with this model, the effect of the heat sub-system on dynamics of the electric sub-system will be studied.

## 3. Steady operating conditions

This section analyzes equilibrium points of the dynamical model (6) in order to investigate the steady operating conditions of the generators. Since the dynamical model (6) has the same formulation as the classical swing equations, the analysis method used in [12] is applied for investigating how the steady state characteristics depend on  $Q'_n$ . From the condition  $d\delta_i/dt = 0$  at equilibrium points, we have

$$\omega_i^* = 0, \quad (7)$$

where  $\omega_i^*$  represents the value of  $\omega_i$  at equilibrium points. From the condition  $d\omega_i/dt = 0$ , the values of phase angles  $\delta_1^*$  and  $\delta_2^*$  satisfy the following equations:

$$\begin{aligned} \alpha_1 &= \sin \delta_1^* + \kappa_1 \sin(\delta_1^* - \delta_2^*) + \lambda_1 \cos \delta_1^* + \mu_1 \cos(\delta_1^* - \delta_2^*), \\ \alpha_2 &= \sin \delta_2^* + \kappa_2 \sin(\delta_2^* - \delta_1^*) + \lambda_2 \cos \delta_2^* + \mu_2 \cos(\delta_2^* - \delta_1^*), \end{aligned} \quad (8)$$

where  $\alpha_1$  and  $\alpha_2$  are defined by

$$\alpha_1 := \frac{\eta_{e1}(Q'_{L1} + Q'_n) - \eta_{h1}E_1^2G_{11}}{\eta_{h1}E_1E_\infty B_{1\infty}}, \quad (9a)$$

$$\alpha_2 := \frac{\eta_{e2}(Q'_{L2} - Q'_n) - \eta_{h2}E_2^2G_{22}}{\eta_{h2}E_2E_\infty B_{2\infty}}, \quad (9b)$$

and  $\kappa_i$ ,  $\lambda_i$ , and  $\mu_i$  are given by

$$\kappa_i = \frac{E_1E_2B_{12}}{E_iE_\infty B_{i\infty}}, \quad \lambda_i = \frac{G_{i\infty}}{B_{i\infty}}, \quad \mu_i = \frac{E_1E_2G_{12}}{E_iE_\infty B_{i\infty}}. \quad (10)$$

By solving the equation (8), the values of  $\delta_1^*$  and  $\delta_2^*$  are numerically determined. Fig. 2 shows the result on existence and number of equilibrium points. The values of parameters are shown in Tab. 1. In the region  $R_n$  ( $n = 2, 4, 6$ ), there are  $n$  distinct equilibrium points. In the three regions, one of the equilibrium points is asymptotically stable, and the others are unstable. The stable equilibrium point represents a synchronized motion of the two generators in which they operate with the same frequency as the infinite bus.

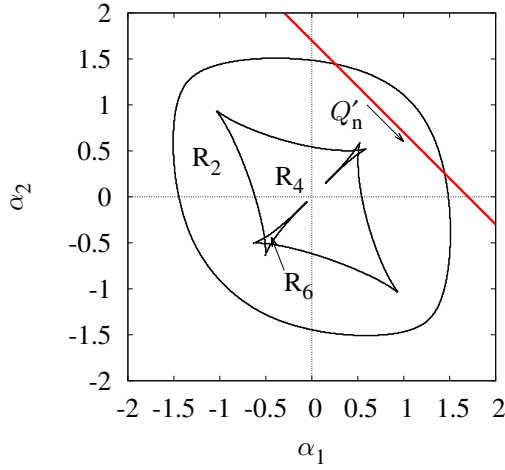


Figure 2: Numerical result on existence and number of equilibrium points. In the region  $R_2$  (or  $R_4$ ,  $R_6$ ), there are two (or four, six) distinct equilibrium points of the dynamical model (6).

Table 1: Values of parameters for numerical analysis

Rated power	$P_b$	1.0 MW
Synchronous speed	$\omega_b$	$2\pi \cdot 60$ Hz
Inertial constant	$H_i$	10 s
Damping coefficient	$D_i$	0.005
Voltage	$E_i$	1.0
Transfer susceptance (# $i$ , $\infty$ )	$B_{i\infty}$	1.0
Transfer conductance (# $i$ , $\infty$ )	$G_{i\infty}$	-0.1
Transfer susceptance (#1, #2)	$B_{12}$	0.5
Transfer conductance (#1, #2)	$G_{12}$	0.05
Transfer conductance (# $i$ , # $i$ )	$G_{ii}$	0.05
Heat load	$Q_{Li}$	0.9
Coefficient of electricity output	$\eta_{ei}$	0.40
Coefficient of heat output	$\eta_{hi}$	0.40

Here, we consider the stability of the equilibrium points due to the quasi-static changes of the parameters of the heat sub-system. As  $Q'_n$  changes, the steady operating point moves in the  $(\alpha_1, \alpha_2)$ -plane along the straight line given by

$$e_1\alpha_1 + e_2\alpha_2 = (Q'_{L1} + Q'_{L2}) - e_3 \quad (11)$$

where the coefficients  $e_1$  to  $e_3$  are determined by the parameters of the electric sub-system and are given by

$$\begin{aligned} e_1 &:= \frac{\eta_{h1}}{\eta_{e1}} E_1 E_\infty B_{1\infty}, & e_2 &:= \frac{\eta_{h2}}{\eta_{e2}} E_2 E_\infty B_{2\infty}, \\ e_3 &:= \frac{\eta_{h1}}{\eta_{e1}} E_1^2 G_{11} + \frac{\eta_{h2}}{\eta_{e2}} E_2^2 G_{22}. \end{aligned} \quad (12)$$

The equation (11) is obtained by eliminating  $Q'_n$  from (9). Since the line (11) is parameterized by  $Q'_{L1} + Q'_{L2}$ , a steady operating condition is determined by the values of  $Q'_n$  and  $Q'_{\text{sum}} := Q'_{L1} + Q'_{L2}$ . In Fig. 2, the red line shows (11) with  $Q'_{\text{sum}} = 1.8$ . The synchronized operation of the generators is achieved when the operating condition determined by  $Q'_n$  and  $Q'_{\text{sum}}$  is kept within  $R_2$ .

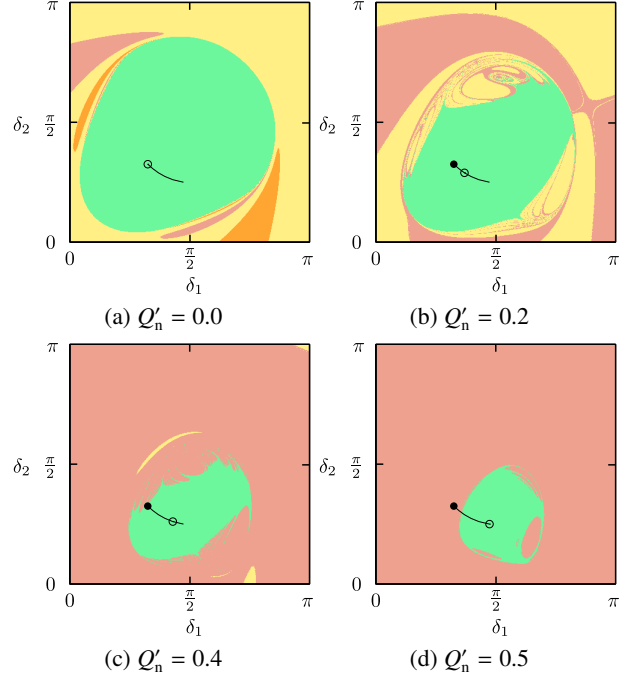


Figure 3: Visualization of basins of attraction. The solid line shows the equilibrium points under various  $Q'_n$  between 0 and 0.5. The circle ( $\circ$ ) shows the equilibrium point for each  $Q'_n$ , and the dot ( $\bullet$ ) for  $Q'_n = 0$ .

#### 4. Basins of attraction

This section analyzes the basins of attraction of the stable equilibrium points under several fixed values of  $Q'_n$ . Based on the analysis, we consider the effect of heat transfer management on the dynamics of the electric sub-system. A possible open-loop control is then discussed in terms of a transient instability. Following [6–8], the basin of attraction is visualized by taking a two-dimensional slice of  $\{(\delta_1, \delta_2, \omega_1, \omega_2) \in \mathbb{X} \mid \omega_1 = 0, \omega_2 = 0\}$  in the entire phase space  $\mathbb{X} := \mathbb{T}^2 \times \mathbb{R}^2$ , where  $\mathbb{T}$  stands for the torus, and  $\mathbb{R}$  for the set of real number. For the slice, initial conditions on a grid of  $401 \times 401$  points were numerically integrated. Each point is colored according to the attractor reached from the corresponding initial condition.

Fig. 3 shows the visualization of the basins of attraction under several values of  $Q'_n$ . Under the current setting of the parameters, the system (6) has four attractors. One attractor is the stable equilibrium point representing the steady operating condition: this is shown by circle ( $\circ$ ) in the figure, and its basin is colored green. A second attractor is a periodic orbit, in which the generator #1 operates at a desynchronized manner with the infinite bus: its basin is colored red. A third one is another periodic orbit, in which the generator #2 is desynchronized; its basin is colored orange. In the fourth attractor, both generators are desynchronized; its basin is yellow. Fig. 3 indicates that the heat transfer management affects the responses of the electric sub-system, and the basins of attraction of the stable

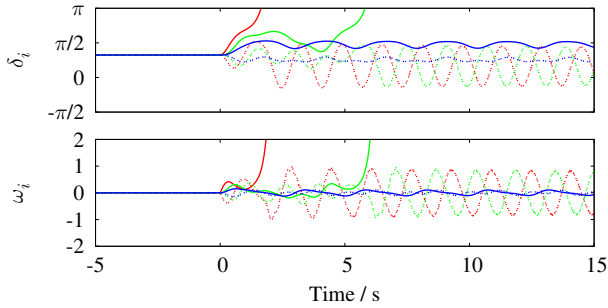


Figure 4: System's responses to ramp-wise changes of the heat transfer rate under  $T_d = 0, 0.5,$  and  $1.0$  s. The *solid* line shows the response of the generator #1, and the *broken* line the generator #2.

equilibrium points become small on the two-dimensional slices as  $Q'_n$  increases. In [2], a similar result is obtained for  $D_i = 0.21$  and  $\lambda_i = \mu_i = 0$ .

This analysis suggests a possibility of instability due to a change of  $Q'_n$ . In Fig. 3, the *solid* line shows the stable equilibrium points under various  $Q'_n$  between 0 and 0.5, and the dot ( $\bullet$ ) the equilibrium point under  $Q'_n = 0$ . The basins of attraction directly illustrates the following two ideal operations of the two-site system. Since there exists an equilibrium point for each  $Q'_n$ , quasi-static change of the set-points of the CHP plants enables the change of operating conditions of the generators along the lines in Fig. 3. However, a step-wise change of  $Q'_n$  from 0 to 5.0 desynchronizes the generator #1 because the dot ( $\bullet$ ) exists outside the domain of attraction of the stable equilibrium point in Fig. 3d.

As a realistic situation, an open-loop control of the heat transfer rate  $Q'_n$  can be considered as in between the above two ideal situations. In this paper, based on [13], we consider a ramp-wise change of the set-points of CHP plants from  $Q'_n = 0$  to 0.5. The duration  $T_d$  of the change of the set-points is an important parameter:  $T_d = 0$  corresponds to the step-wise change, and  $T_d = \infty$  the quasi-static change. In an engineering viewpoint, the range of  $T_d$  where the instability does not occur is of significant importance. Fig. 4 shows the system's responses for  $T_d = 0, 0.5,$  and  $1.0$  s. The *red* line shows the case of  $T_d = 0$  (step-wise change), and the generator #1 is desynchronized as mentioned above. In the case of  $T_d = 1.0$  s (*blue* line), the variables  $\delta_i$  and  $\omega_i$  converged to the values of the equilibrium point. In the case of  $T_d = 0.5$  s, it is observed that the generator #1 is desynchronized. The analysis of the relationship between  $T_d$  and the basins of attraction is future work and discussed at the end of this paper.

## 5. Conclusions and discussion

In this paper, we analyzed the basins of attraction of equilibrium points representing steady operating conditions of synchronous generators in a two-site electricity and heat supply system. The slices of the basins were visualized under various fixed values of heat transfer rate  $Q'_n$ .

The analysis indicated that the heat transfer management affected the responses of the electric sub-system, and the basin of attraction of the stable equilibrium point became small depending on  $Q'_n$ . Furthermore, a possibility of instability was discussed for step-wise and ramp-wise changes of the set-points of the CHP plants. It was observed that the instability possibly occurred under a ramp-wise change with a small values of the duration  $T_d$ .

Finally, for the future work, we discuss the possibility of analyzing  $T_d$  via the basins of attraction. After the time  $t = T_d$ , from the uniqueness of the solution of (6), the resultant behavior is determined by the basins in Fig. 3 if the state trajectory passes the slice determined by  $\omega_1 = \omega_2 = 0$ . However, in general, this is not the case because the two dimensional slice is not transversal in the full four-dimensional phase space. Nevertheless, it is observed in the case of  $T_d = 0.5$  s (green line) in Fig. 4 that the state passes a slice of  $\{(\delta_1, \delta_2, \omega_1, \omega_2) \in \mathbb{X} \mid \omega_1 = \epsilon, \omega_2 = 0\}$  for a small  $\epsilon$ . Thus, if the basin structure does not vary drastically depending on the values of  $\omega_i$ , the visualization of the basins in Fig. 3 may be used for the analysis.

## References

- [1] H. Hoshino, Y. Susuki, and T. Hikiyara, *Proc. 2014 Int. Symp. Nonlinear Theory and its Application*, pp. 482–485, 2014.
- [2] H. Hoshino, Y. Susuki, and T. Hikiyara, *Trans. of ISCIE*, vol. 27, no. 11, pp. 452–460, 2014 (in Japanese).
- [3] H. Hoshino, Y. Susuki, T. J. Koo, and T. Hikiyara, *Proc. the 60th Annual Conference of ISCIE*, 141–4, 2016.
- [4] A. Isidori, *Nonlinear Control Systems, 3rd ed.*, Springer, 1995.
- [5] S. Sastry, *Nonlinear Systems: Analysis, Stability and Control*. Springer, 1999.
- [6] Y. Ueda, T. Enomoto, and H. B. Stewart, *Applied Chaos*, pp. 207–218, 1992.
- [7] Y. Ueda, Y. Ueda, and H. B. Stewart, *Int. J. Bifurcat. Chaos*, vol. 8, no. 6, pp. 1183–1197, 1998.
- [8] Y. Hasegawa and Y. Ueda, *Int. J. Bifurcat. Chaos*, vol. 9, no. 8, pp. 1549–1569, 1999.
- [9] C. S. Hsu, *Cell-to-Cell Mapping: A Method of Global Analysis for Nonlinear Systems*, Springer-Verlog, 1987.
- [10] J. Machowski, J. W. Bialek, and J. R. Bumby, *Power System Dynamics: Stability and Control, 2nd ed.* John Wiley & Sons, 2008.
- [11] F. P. de Mello and D. Ahner, *IEEE T. Power Syst.*, vol. 9, no. 3, pp. 1698–1708, 1994.
- [12] A. Arapostathis and P. Varaiya, *Int. J. Electric. Power*, vol. 5, no. 1, pp. 22–30, 1983.
- [13] W. I. Rowen, *J. Engineering for Power*, vol. 105, no. 4, pp. 865–869, 1983.